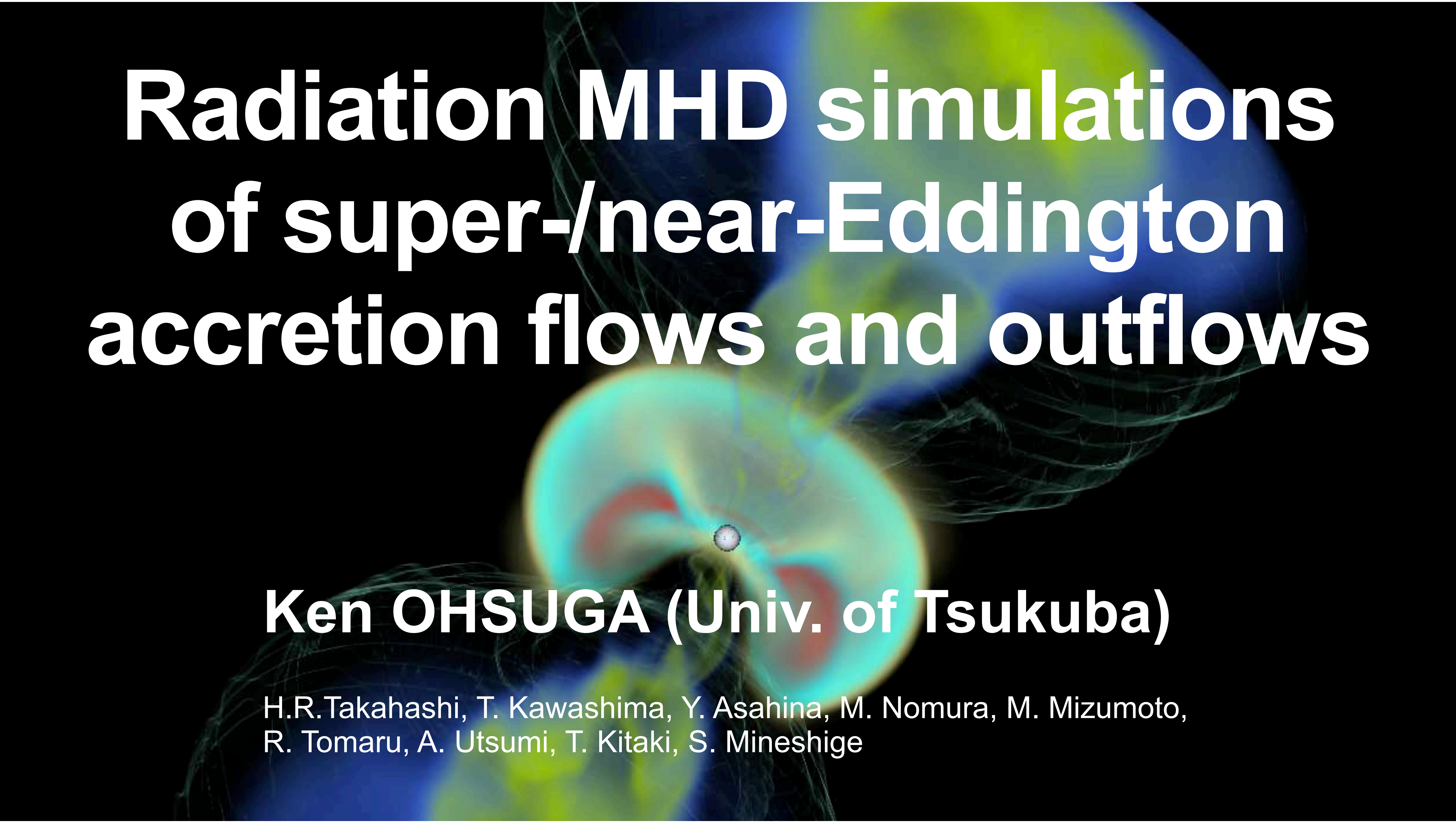

Radiation MHD simulations of super-/near-Eddington accretion flows and outflows

Ken OHSUGA (Univ. of Tsukuba)

H.R.Takahashi, T. Kawashima, Y. Asahina, M. Nomura, M. Mizumoto,
R. Tomaru, A. Utsumi, T. Kitaki, S. Mineshige

Three Accretion Modes

Different spectral states imply the
existence of different accretion modes

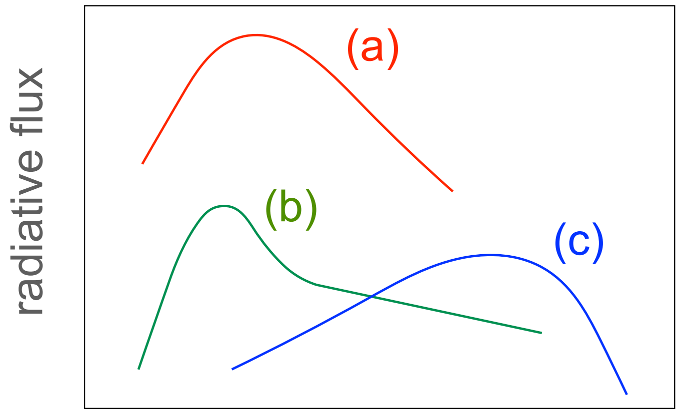

Mass accretion rate
(disk luminosity)

	(a)Slim disk	(b)Standard disk	(c)RIAF/ADAF
			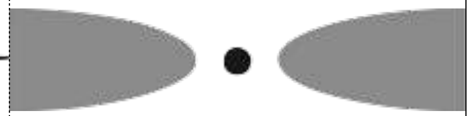
Temperature (10Msun)	~10^8K	~$10^{6\text{-}7}$K	10^9K
Optical thickness	thick	thick	thin

Shakura & Sunyaev 73, Ichimaru 77, Abramowicz et al. 88, Narayan & Yi 1995

BH Mass vs Accretion rate

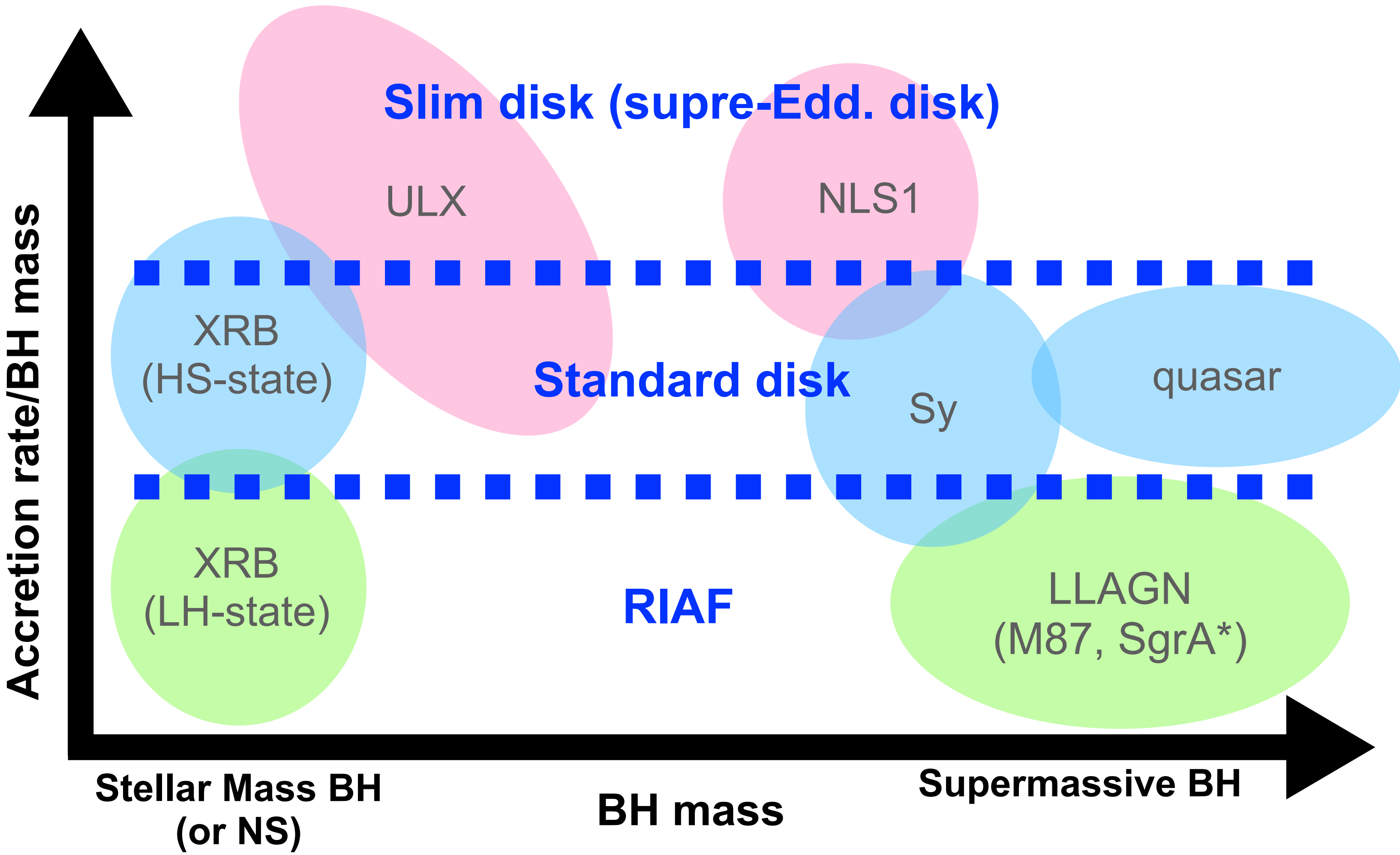

(c)Kawashima

Importance of Radiation and Magnetic Fields

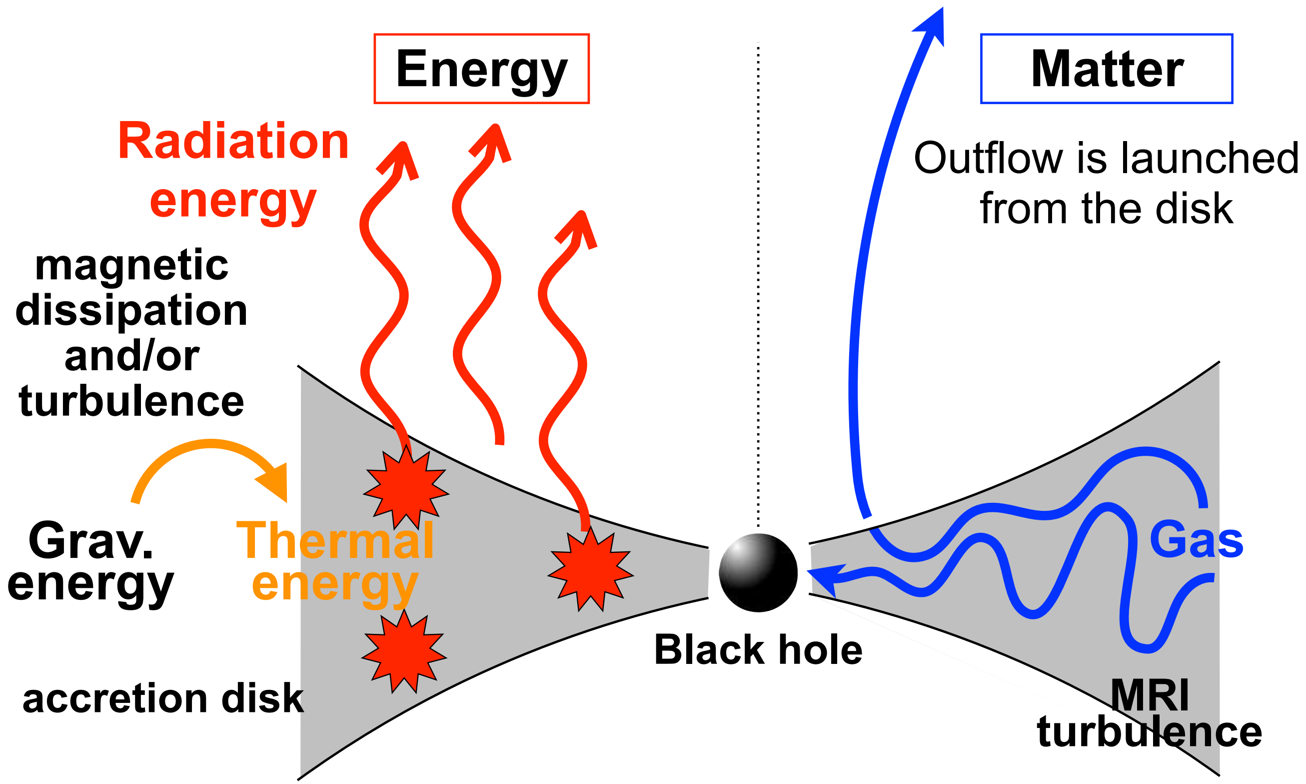

Magnet Fields;

- Angular momentum is transported by MRI, leading to the **mass accretion** onto BHs.

Radiation Fields;

- Disk loses the energy by emitting photons (**cooling**).
- Radiation pressure determines the thickness of the disk.
- Radiation force drives **outflows**

Radiation-MHD Simulations are necessary.

Basic Equations of Radiation-MHD

MHD

mass cons. $$\partial_t\left(\sqrt{-g}\rho u^t\right)+\partial_i\left(\sqrt{-g}\rho u^i\right)=0$$

Gauss's law $$\partial_i\left(\sqrt{-g}B^i\right)=0$$

Gas-Radiation interaction

Induction eq. $$\partial_t\left(\sqrt{-g}B^i\right)=-\partial_j\left[\sqrt{-g}\left(b^j u^i-b^i u^j\right)\right]$$

energy momentum cons. for MHD $$\partial_t\left(\sqrt{-g}T^t_\nu\right)+\partial_i\left(\sqrt{-g}T^i_\nu\right)=\sqrt{-g}T^\kappa_\lambda\Gamma^\lambda_{\nu\kappa}+\sqrt{-g}G_\nu$$

energy momentum cons. for radiation $$\partial_t\left(\sqrt{-g}R^t_\nu\right)+\partial_i\left(\sqrt{-g}R^i_\nu\right)=\sqrt{-g}R^\kappa_\lambda\Gamma^\lambda_{\nu\kappa}-\sqrt{-g}G_\nu$$

RADIATION

We use Kerr-shild metric & M1-closure

They are general relativistic (GR) version; non-GR version is also used.

Radiation-MHD simulations of Super-Edd. Flows

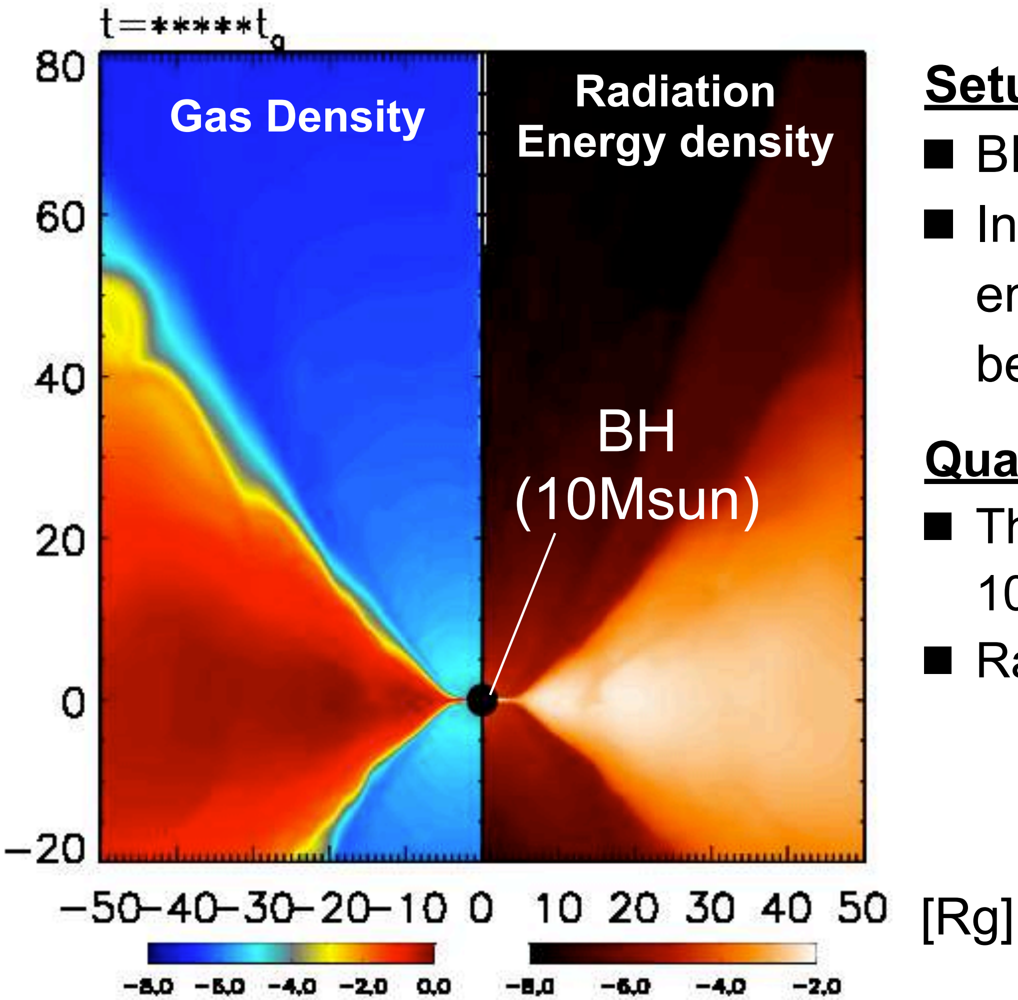

Takahashi, Ohsuga et al. 2016

Setup

- BH mass: 10Msun
- Initial condition: equilibrium torus with embedded poloidal magnetic field (plasma-beta=100)

Quasi-steady structure

- The super-Eddington disks (Mdot ~ a few $100L_{Edd}/c^2$, Ldisk >> L_{Edd})
- Radiatively-driven outflows

see also
Ohsuga et al. 2009; 2011
Sadowski et al. 2014, Jiang et al. 2014

Radiation-MHD simulations of Super-Edd. Flows

Takahashi, Ohsuga et al. 2016

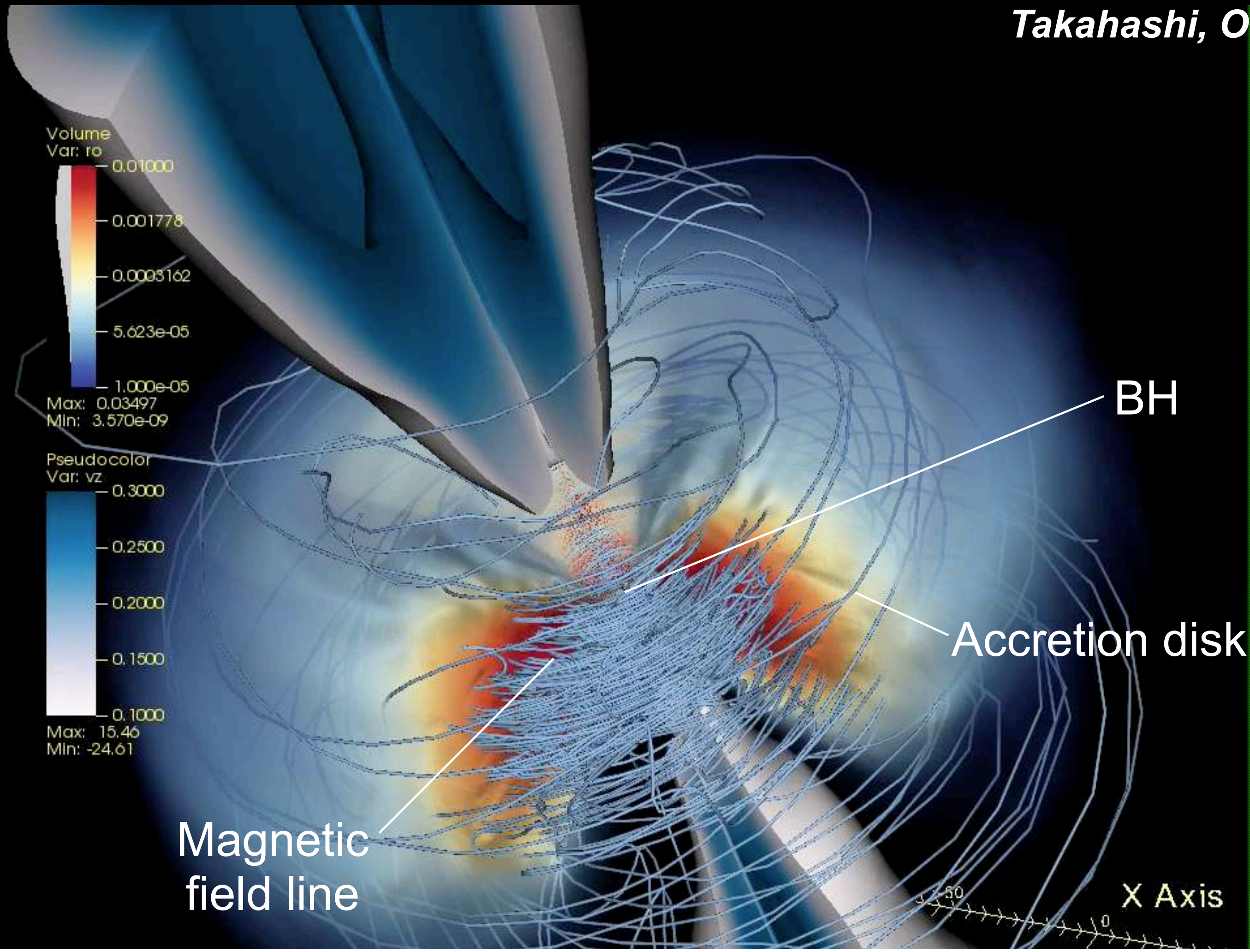

Why is super-Eddington accretion feasible?

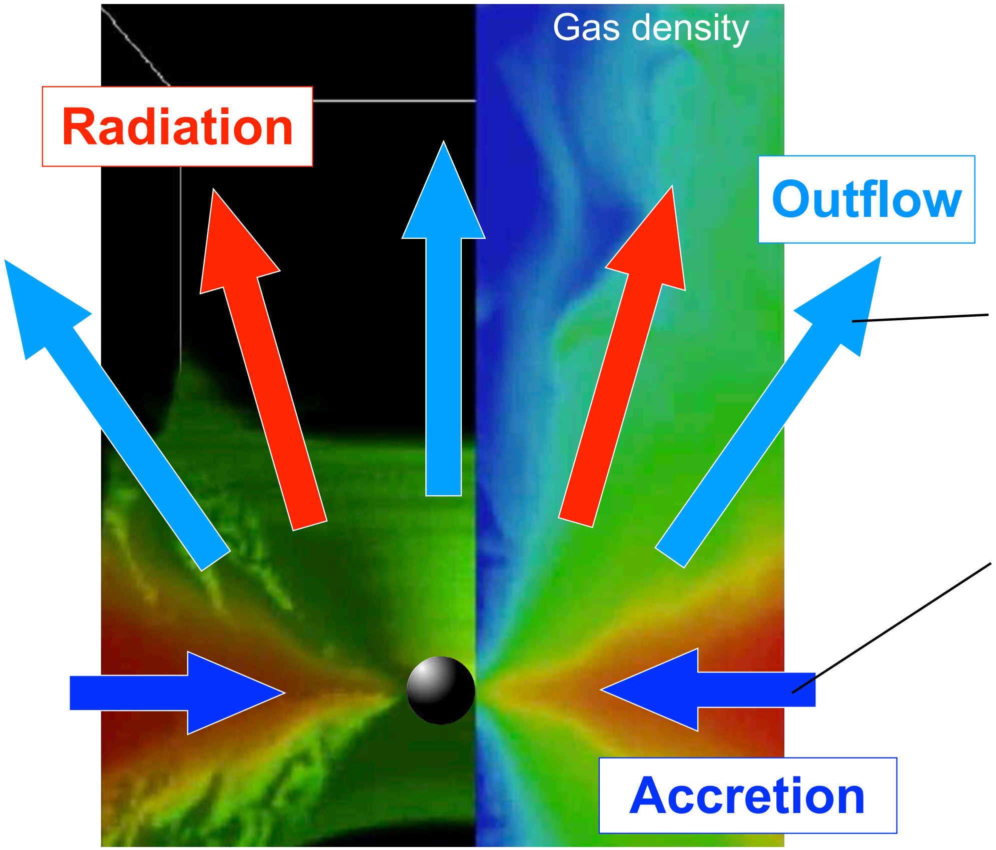

Radiatively driven outflows:
Strong radiation pressure supports the thick disk and generates the outflows above the disk.

Accretion:
Photons mainly escape through the less-dense region above the disk. The radiation pressure cannot prevent the accreting motion within the disk.

Velocity of radiatively-driven outflows (~0.3-0.5c)

Resulting jet velocity (~0.3-0.5c) is roughly consistent with the jets in SS433.

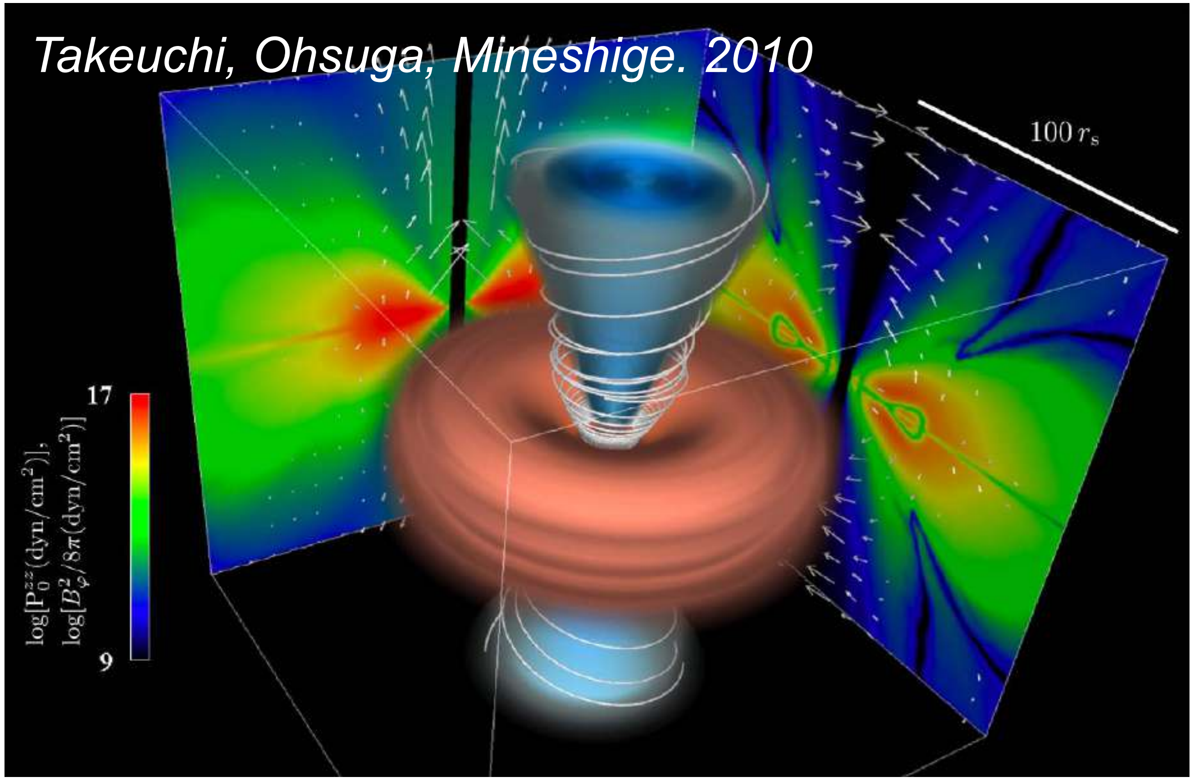

Acceleration via Radiation Flux Force

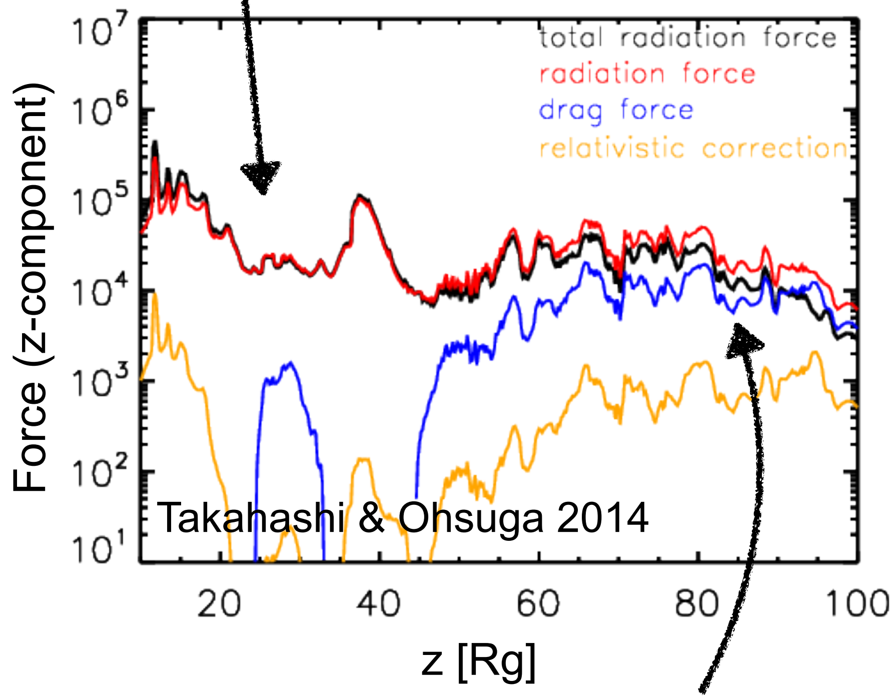

No acceleration because of Flux Force ~ Drag Force

X-RAY SPECTRA

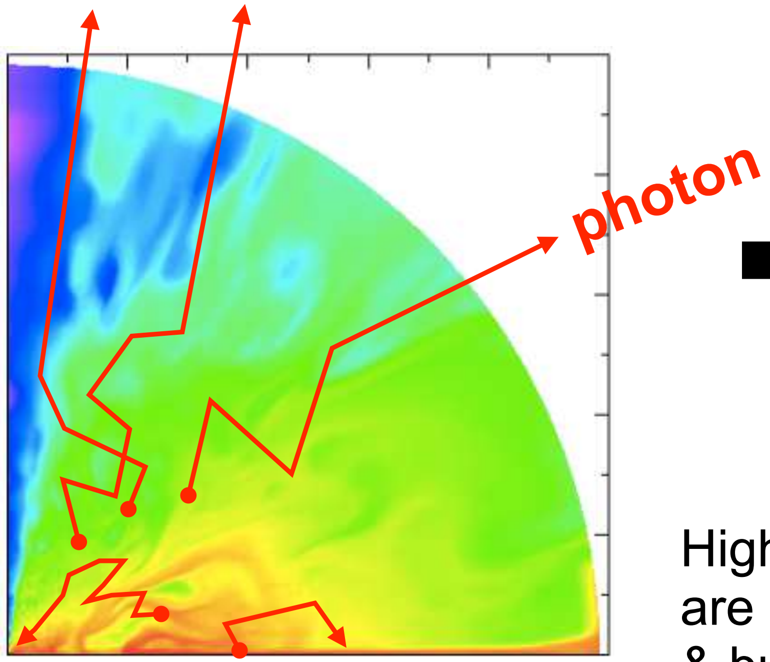

Monte Carlo
Radiation Transfer:

High-energy X-ray photons are produced by the thermal & bulk Comptonization. Simulated spectra nicely fit the observations of ULXs.

Kawashima et al. 2012
(data; Gladstone 2009)

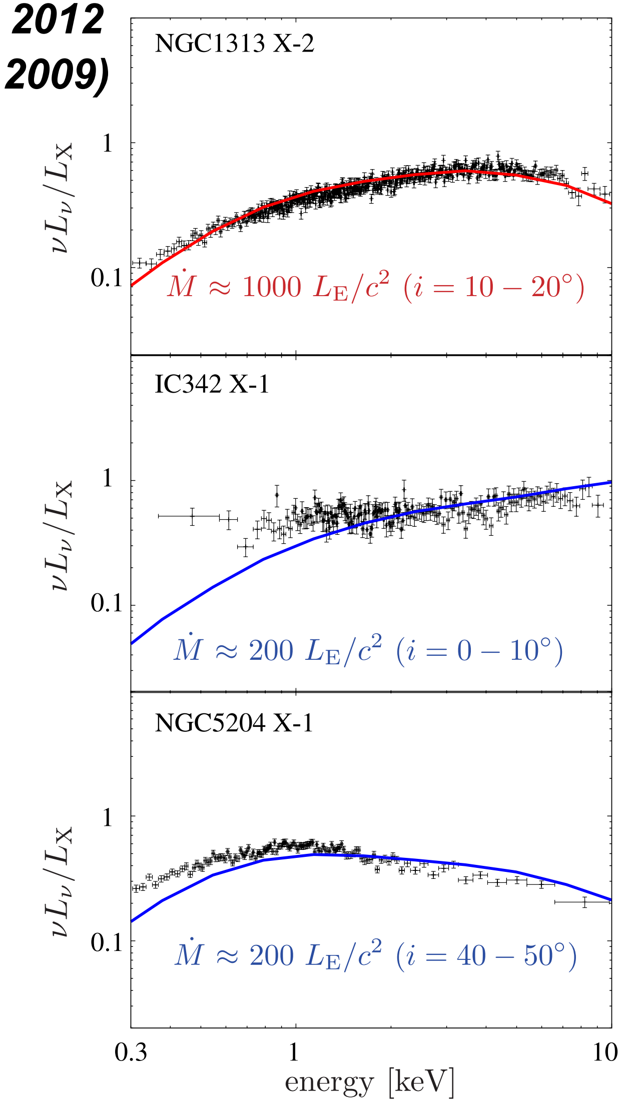

Clumpy outflows from super-Edd. disks

Takeuchi, Ohsuga, Mineshige 2013

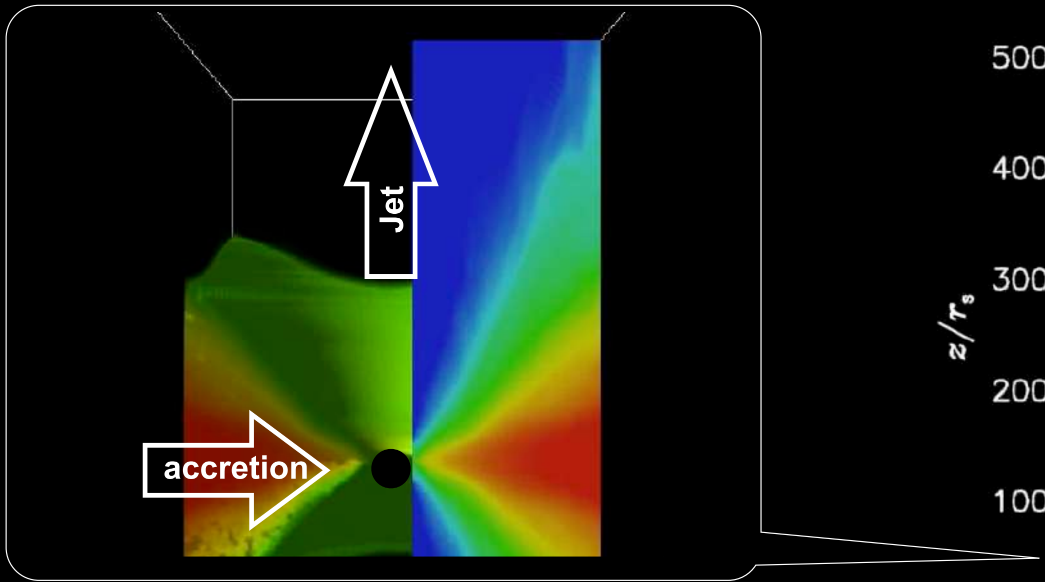

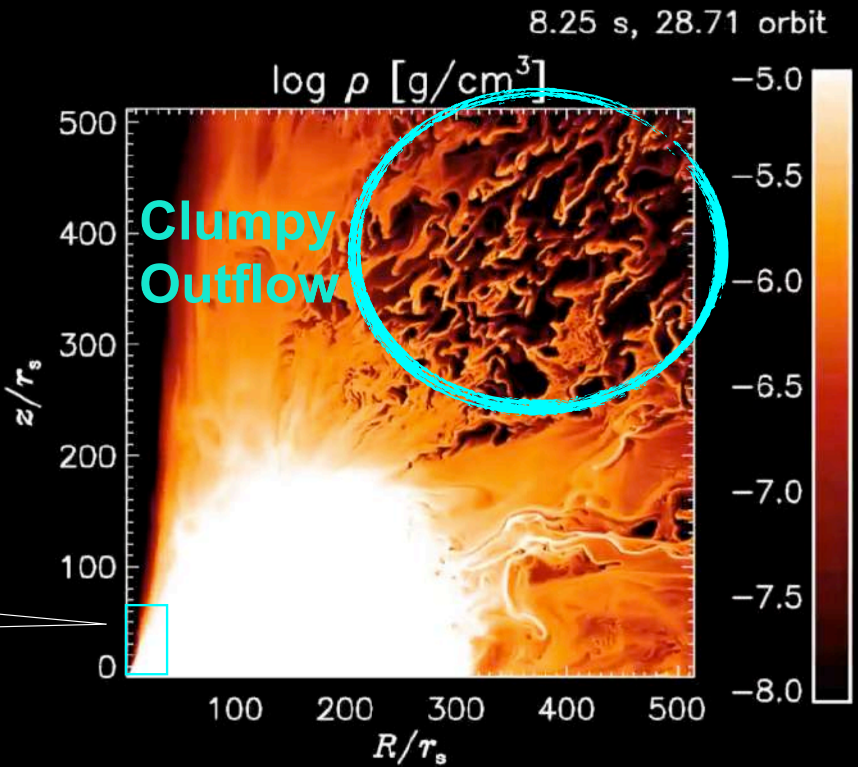

Clumpy outflows: Wind outflows fragment into many gas clouds

RT instability

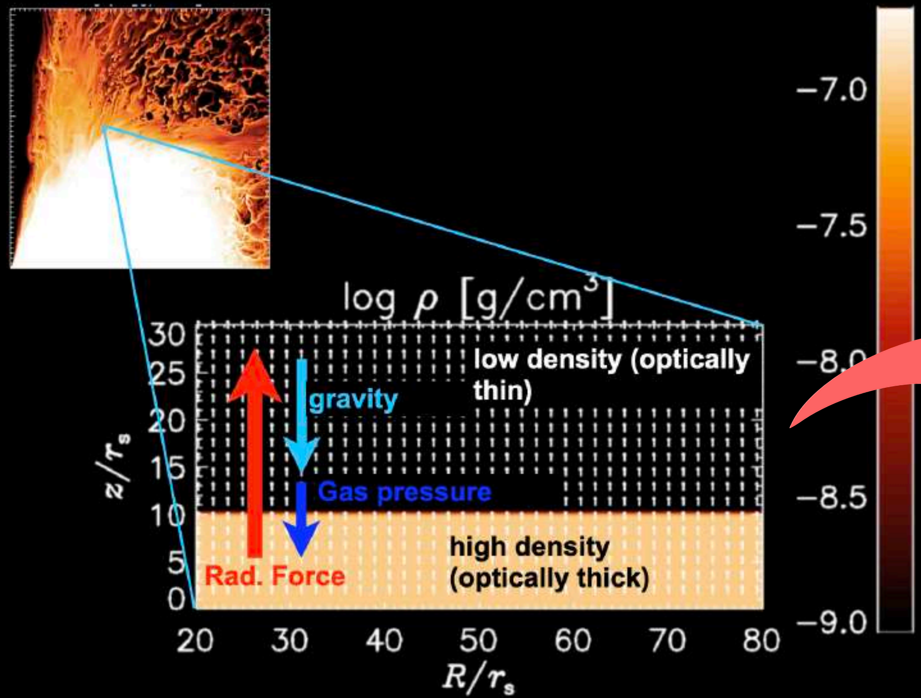

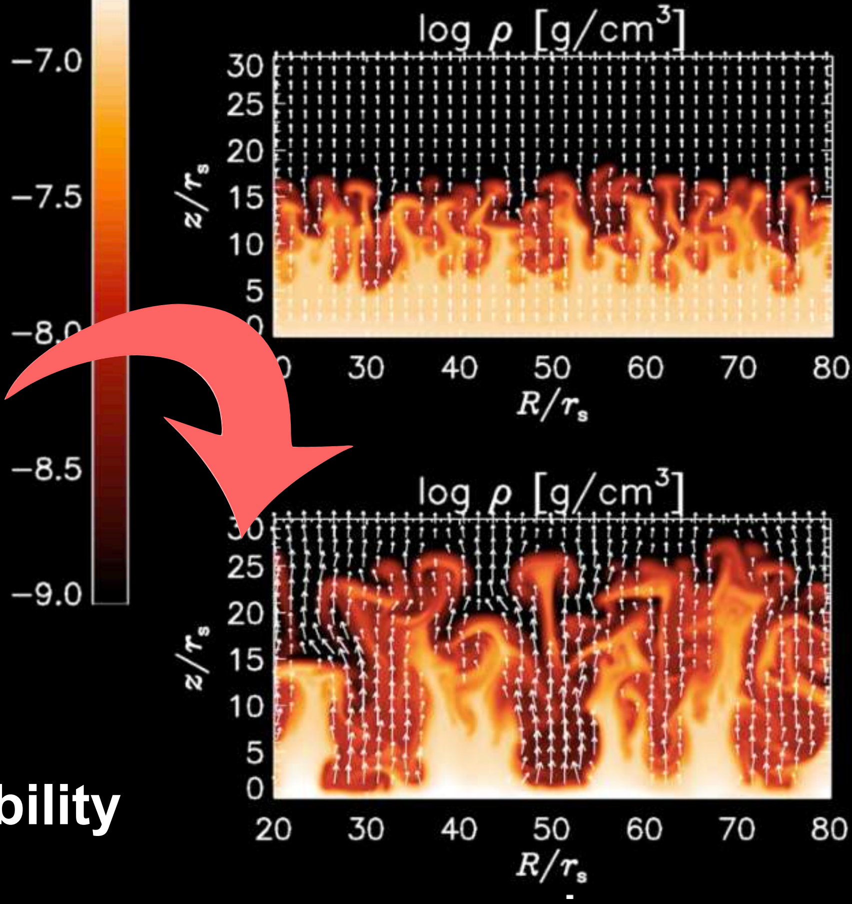

Fragment is caused by the RT instability

Observations of clumpy outflows

Some ULXs exhibit the time variations of X-ray luminosity, implying the launching of clumpy outflows.

Launching of clumpy winds is also reported by observations of NLS1s or V404 Cyg.

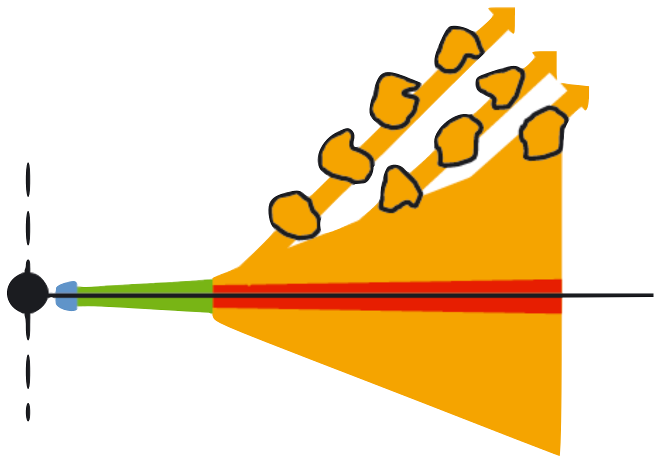

Middleton+11

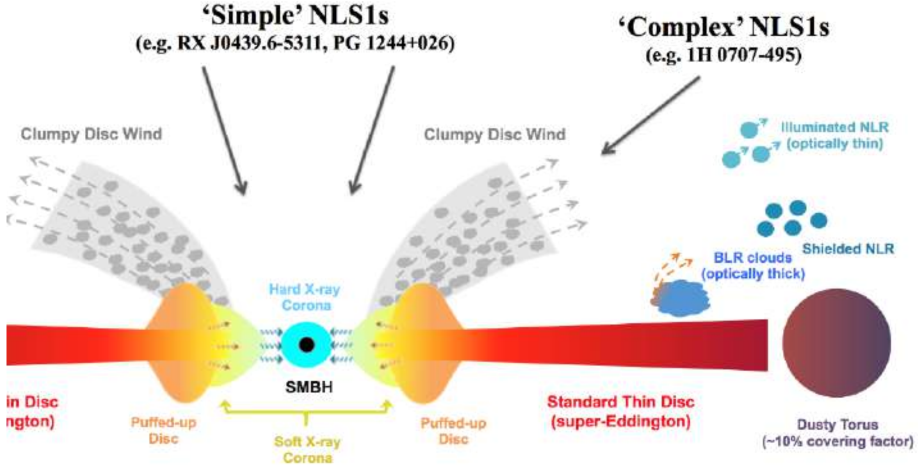

Jin+17 see also Motta+17

Comparison with ULXs *Kobayashi et al. 2018*

Absorption lines

Outflow velocity of ~0.1-0.2c agrees with the observations of blueshifted absorption lines.

Pinto+16,
see also Kosec+18

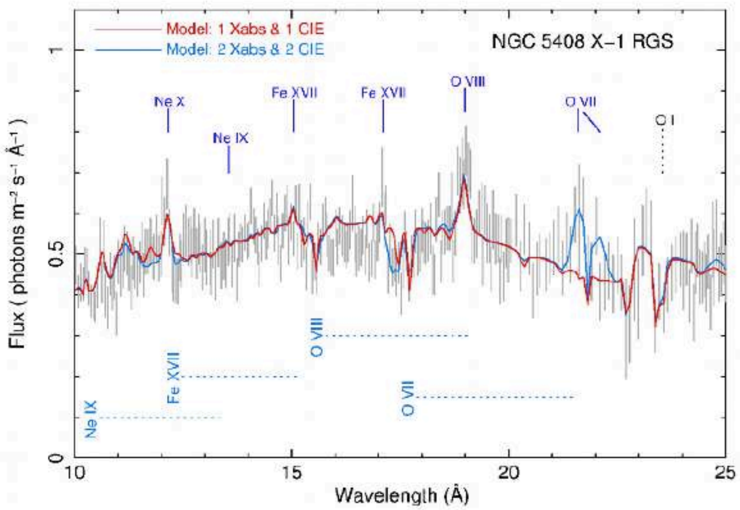

Time variation

Timescale of the luminosity variation (100Rs/0.3V_{kep}) is

$$\sim 2.5 \left(\frac{M_{\rm BH}}{10\ M_\odot}\right)\left(\frac{\ell_{\rm cl}^{\theta}}{10^2\ r_{\rm S}}\right)\left(\frac{r}{10^3\ r_{\rm S}}\right)\ {\rm s}$$

Our result is consistent with the observations of ULXs (Middleton+11) and V404 Cyg (Motta+17) in the case of **M_{BH}~10-100Msun**.

Overall structure of the super-Edd. disk

Schematic picture of the overall structure

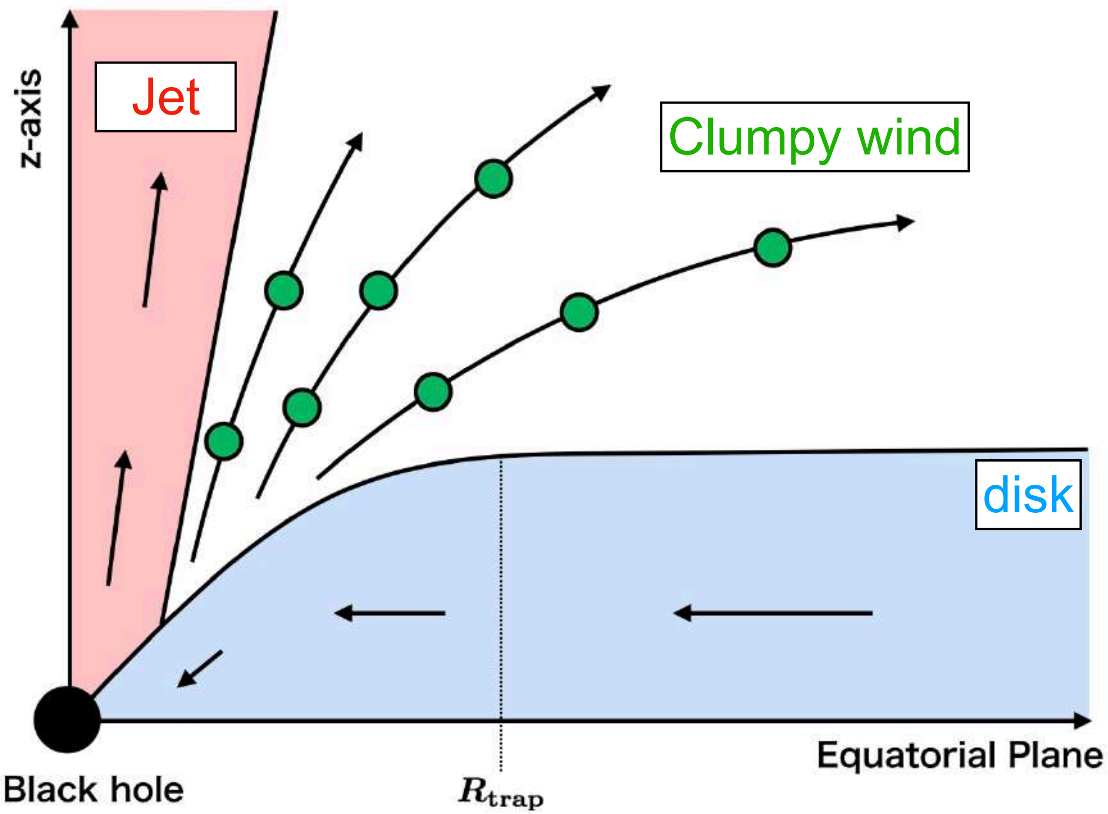

Kitaki et al. 2021, Yoshioka et al. 2022

- Super-Eddington flows consist of three components; radiation pressure-dominated disk, radiatively-driven high-velocity outflow around the rotation axis (jet), radiatively-driven clumpy disk wind.
- High-energy photons are generated by Compton scattering and time variation of the X-ray luminosity is caused by the clumps.

Super-Eddington flows around rotating BH

Utsumi, et al. 2022

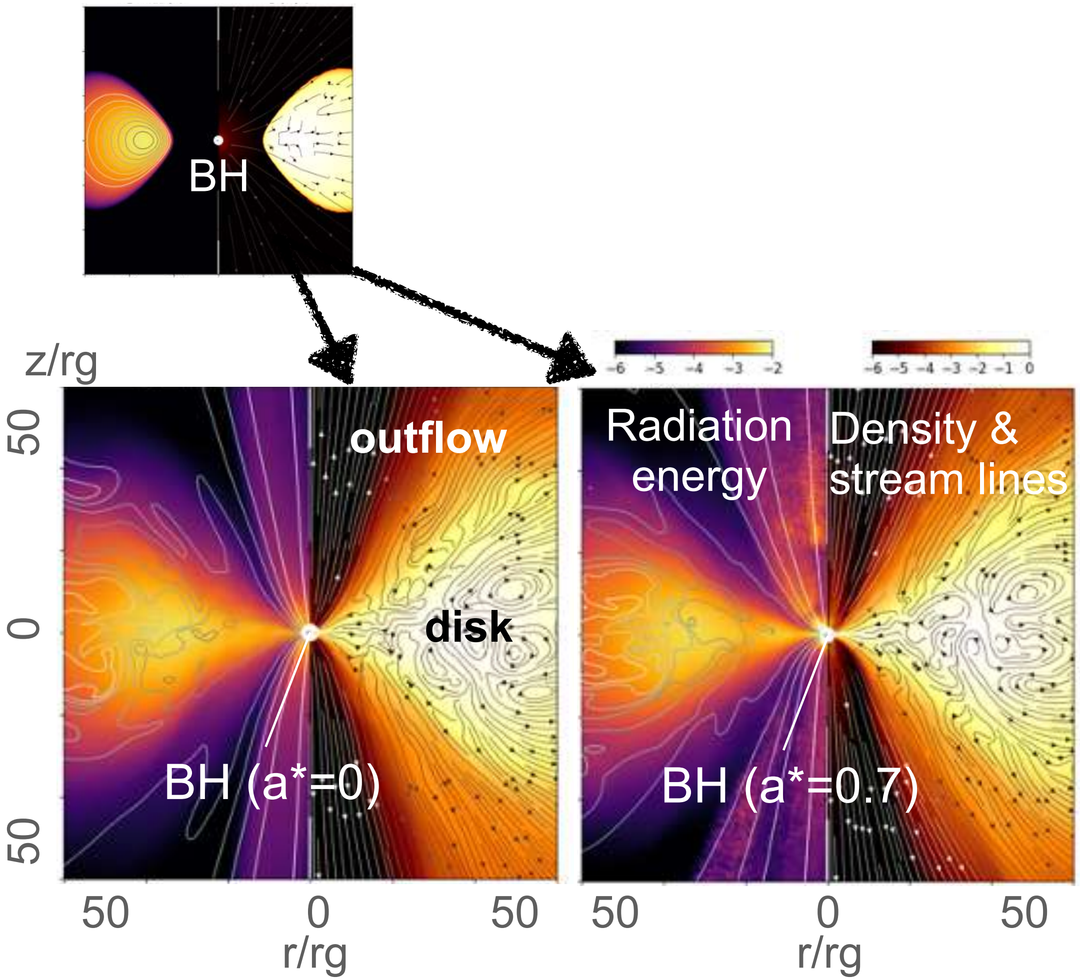

Setup

- BH mass: 10Msun
- Initial condition: equilibrium torus with embedded poloidal magnetic field (plasma-beta=100)
- Spin parameter: -0.9, -0.7, -0.5, -0.3, 0, 0.3, 0.5, 0.7, 0.9

Quasi-steady structure

- In all models, the super-Eddington disks (Mdot ~ a few $100 L_{Edd}/c^2$) and strong outflows are formed.

* Magnetic field is not so strong (SANE)

Energy conversion efficiency

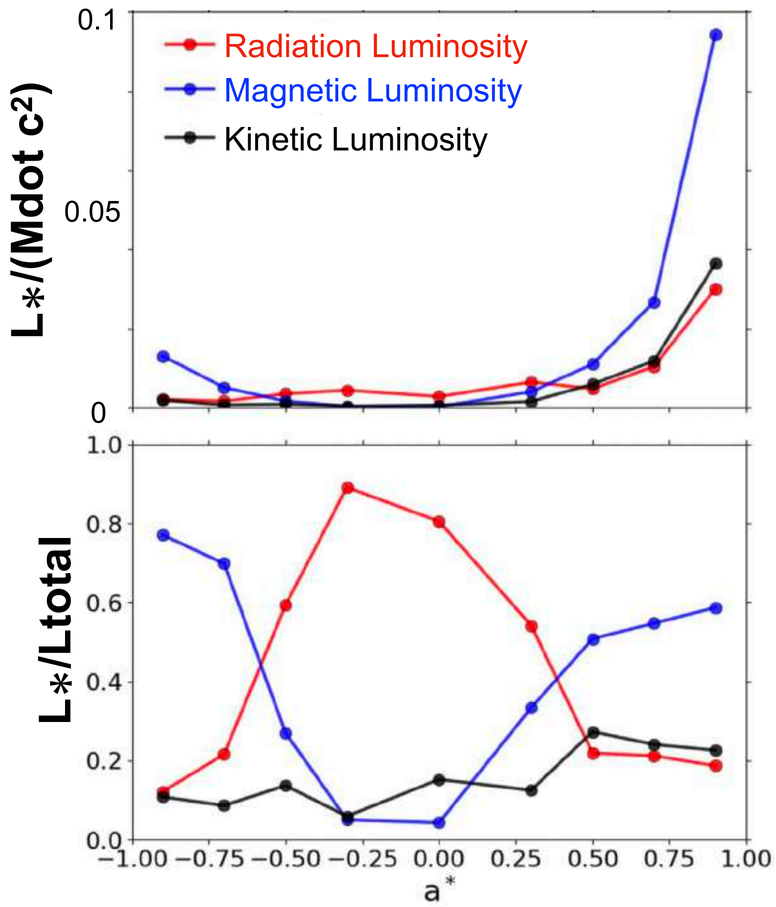

For the case of a*~0, energy is mainly released by the radiation. When |a*| is large, the energy released by the Poynting flux (Magnetic Luminosity) exceeds the Radiation Luminosity.

Radiation luminosity accounts for 80% when a* ~ 0. But the magnetic luminosity is three times larger than the radiation luminosity for the case of a* > 0.5.

see also Sadowski et al. 2014

Enhancement of Poynting flux

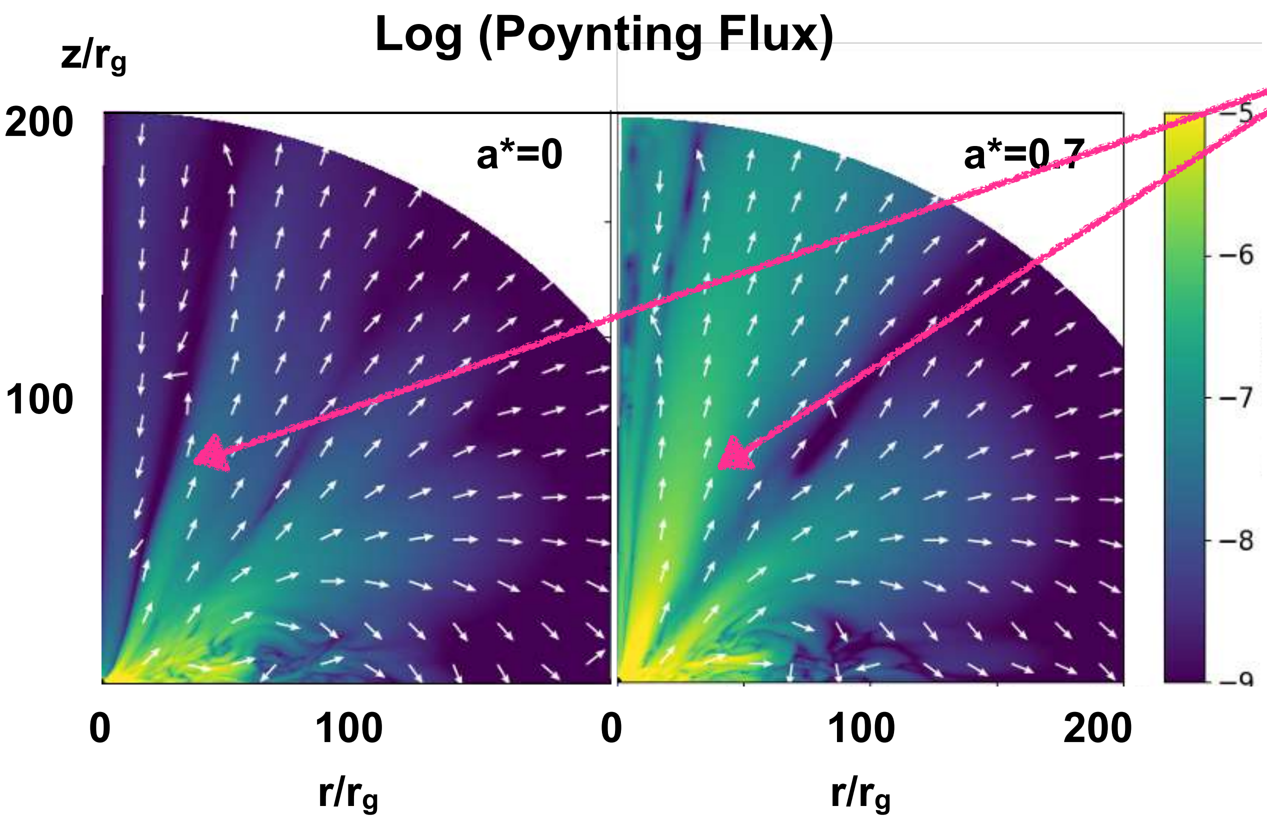

The Poynting flux around the rotation axis is stronger for larger |a*|. This is probably caused by **BZ effect.**

Lense-Thirring precession of super-Edd. disk

Asahina, Ohsuga, submitted

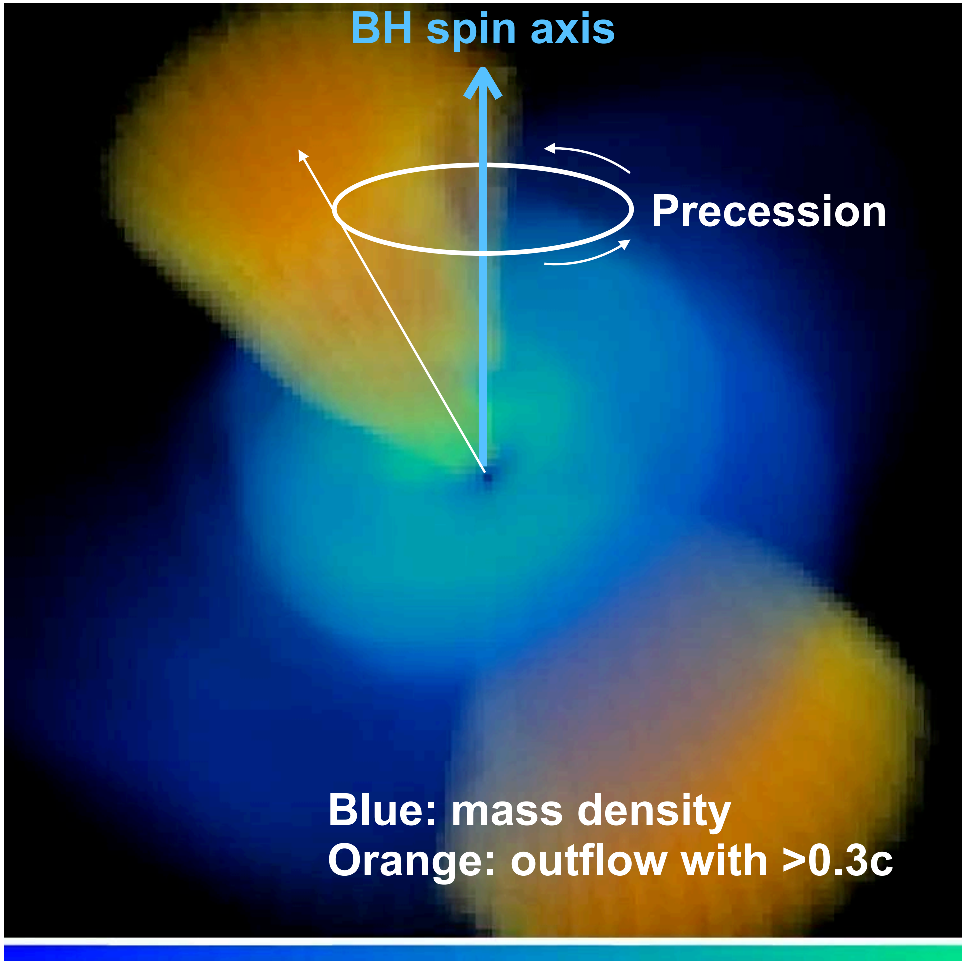

Setup

- BH mass: 10Msun
- Initial condition: equilibrium torus with embedded poloidal magnetic field (plasma-beta=100) tilted 30 degree.
- Spin parameter: 0.9

Inflow-outflow structure

- The super-Eddington disk, which is tilted and twisted, forms.
- Strong outflows are also formed.

- Accretion rate: several 100 L_{Edd}/c^2
- Radiation Luminosity: several L_{Edd}
- Kinetic Luminosity: several L_{Edd}

Tilted and twisted super-Edd. disk

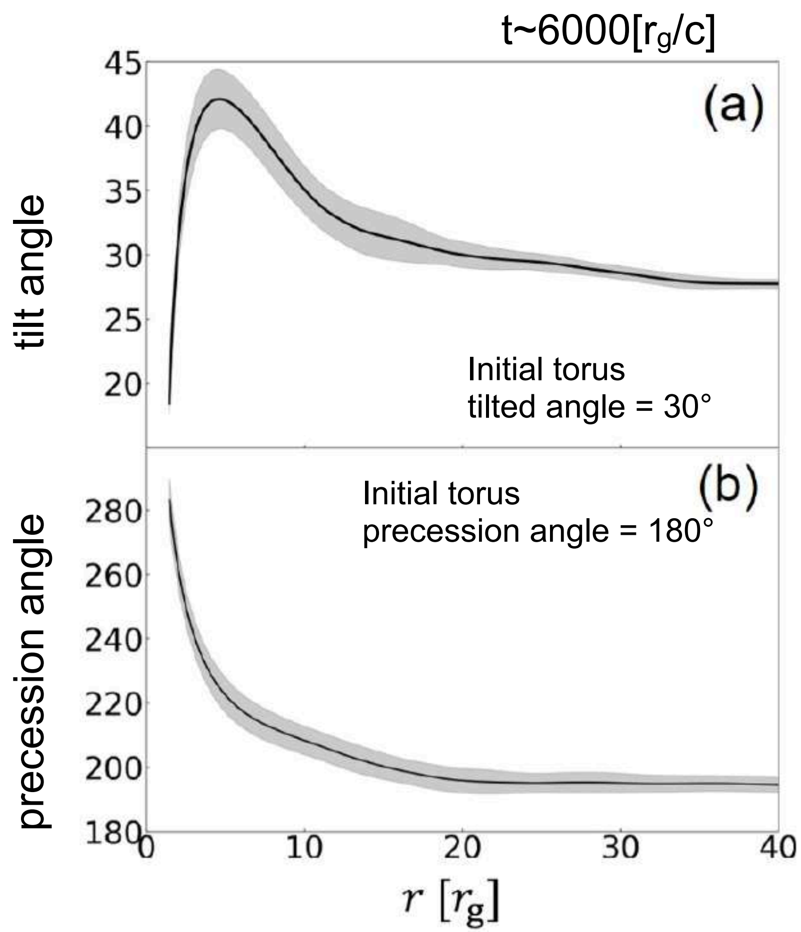

- The tilt angle of the outer region is ~30°, which is determined by the initial setting of the torus.
- The tilt angle as well as the precession angle increases as decrease of the radius => the inner part of the disk is more tilted and more twisted (see below)

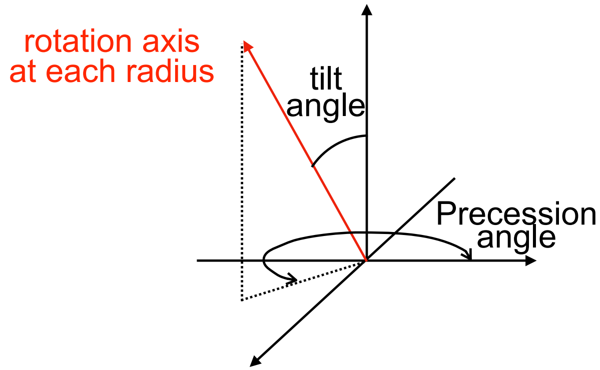

Schematic picture of twisted, tilted disk

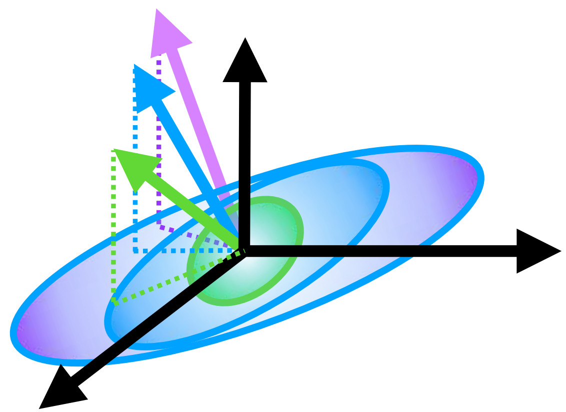

Precession of disk

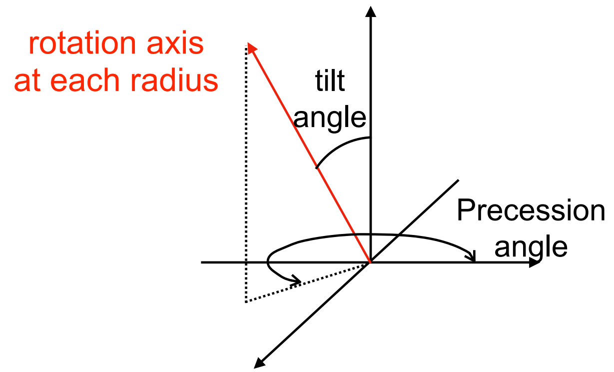

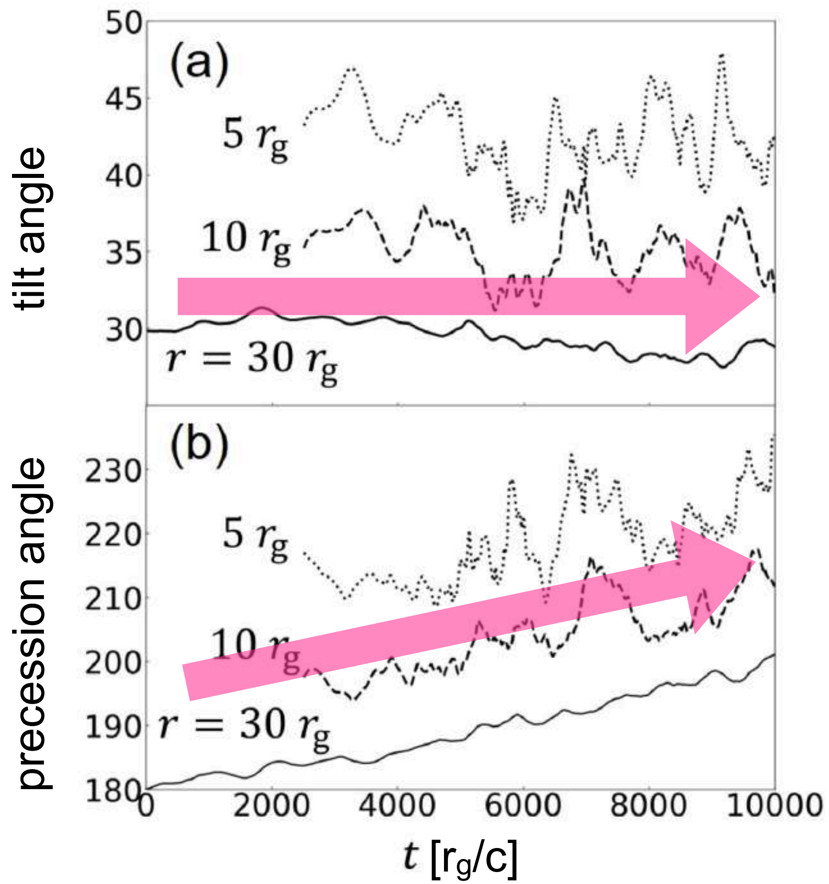

The tilt angle does not change so much.

The precession angle increases with time.

→ The disk exhibits precession motion without changing shape.

*Note that computation time is short.

Precession of outflow & radiation

Ejection direction of outflow and radiation

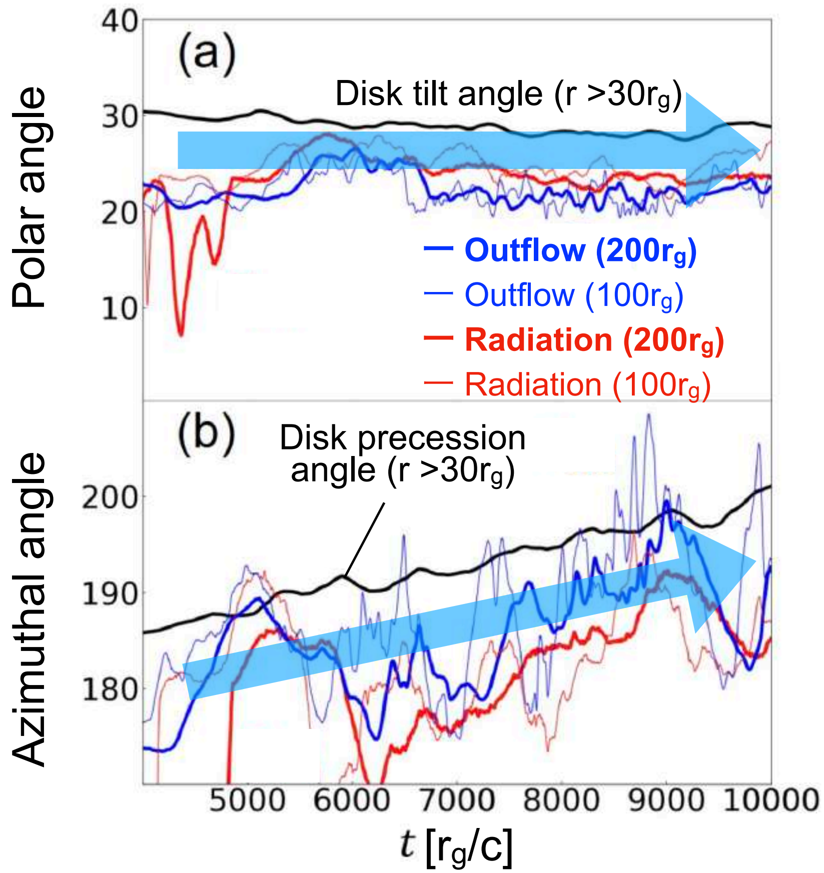

Outflow and radiation are ejected mainly around the disk rotation axis (~30°) and not around the BH spin axis (=0°).

The direction of outflow and radiation increases with time. This is probably caused by the precessional motion of the disk.

The typical timescale of the precession is ~9sec for the case of stellar mass BH(10Msun). **This timescale is consistent with the QPOs observed in some ULXs.**

Simulations of line winds from near-Edd. disks

Nomura et al. 2016, 2017, 2020, 2021
(see also Proga et al. 00, 04)

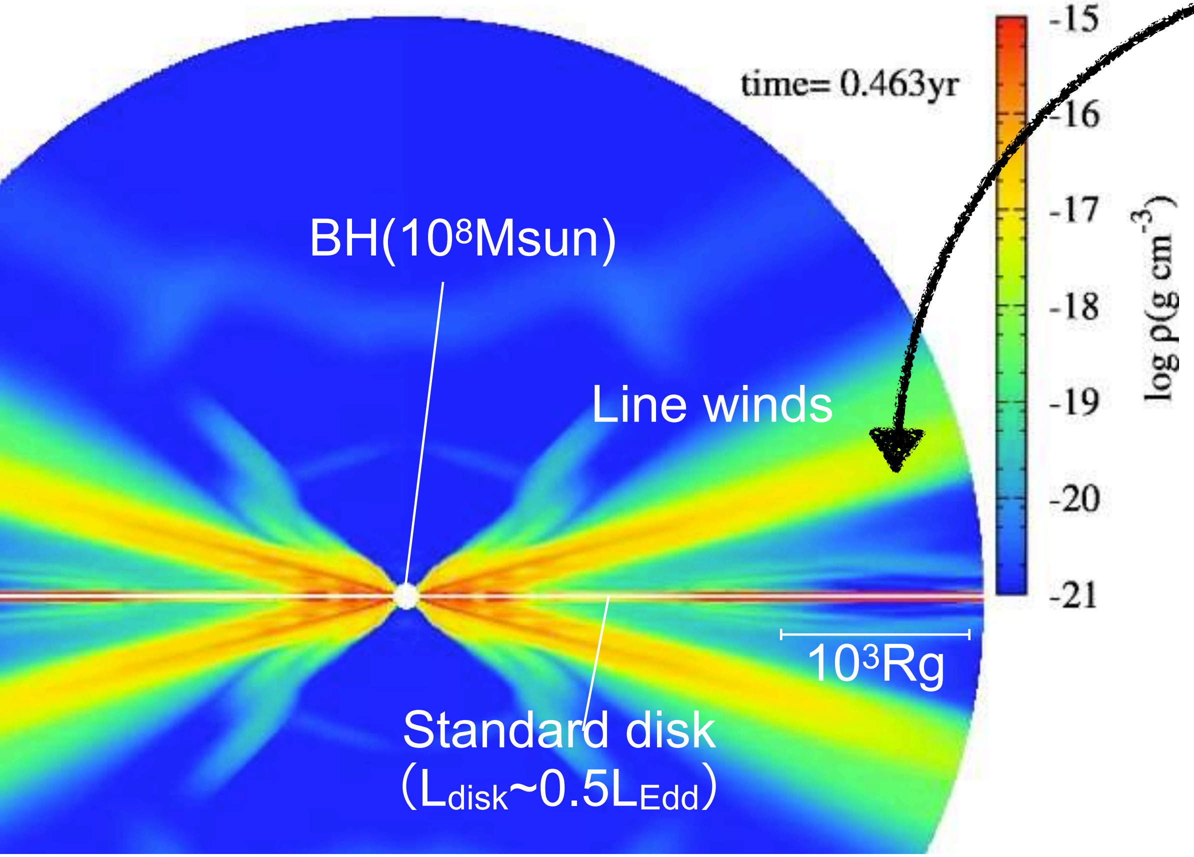

From the standard disk, the disk wind is launched by the radiation force for spectral lines (line-force).

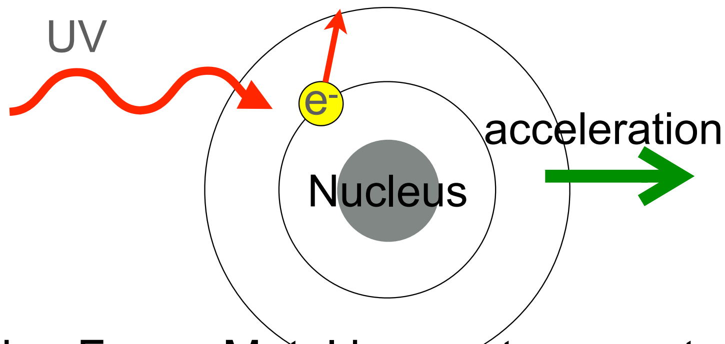

Line Force: Metal ions get momentum by the line absorption (bound-bound transition) of UV.

Comparison with UFOs (PG 1211+143)

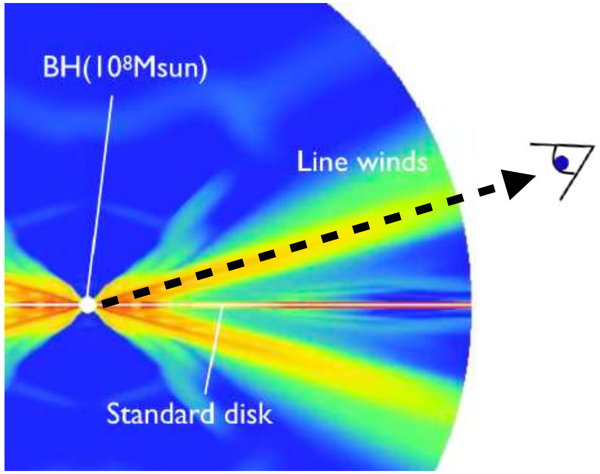

Monte Carlo Radiation Transfer (MONACO):

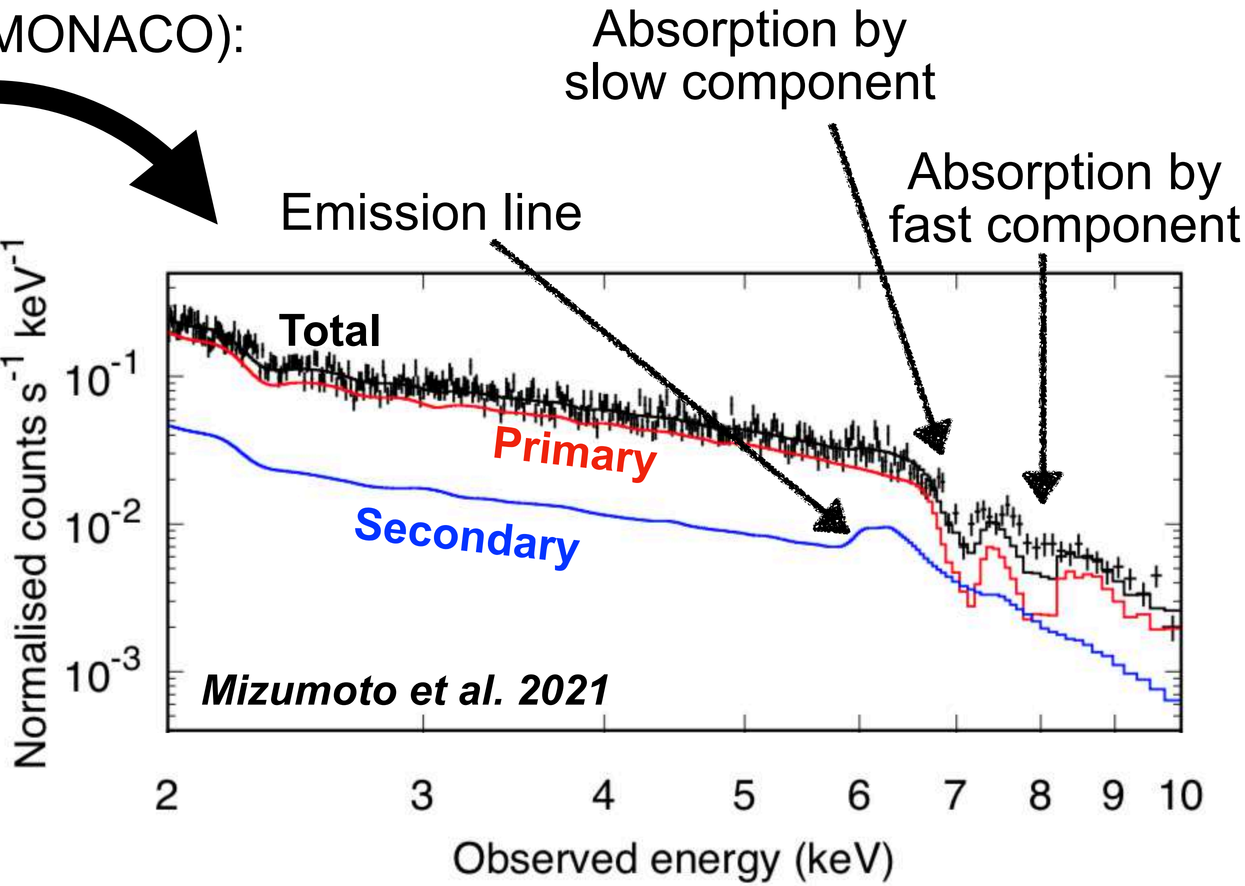

- There are some absorbing regions along the line of sight.
- X-ray spectrum (two absorption lines and emission line) can be well described by our model.

Future observations

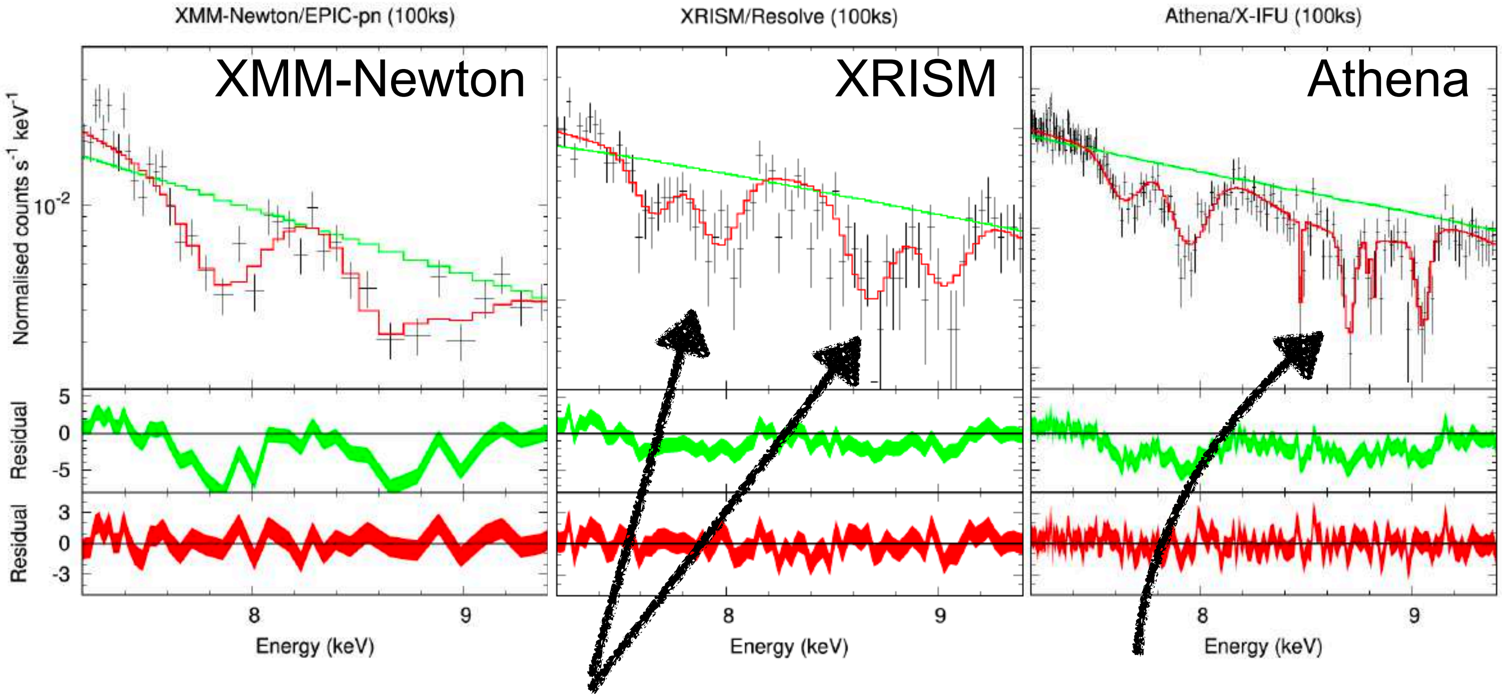

Absorption lines from H-like and He-like iron are resolved by XRISM.

More detailed absorption profiles can be understood by Athena.

A more detailed comparison with observations by XRISM and Athena provides a more accurate understanding of the disk wind structure.

Simulations of thermal-radiative wind from near-Edd. disks

Tomaru et al. 2020

Number Density (log n)

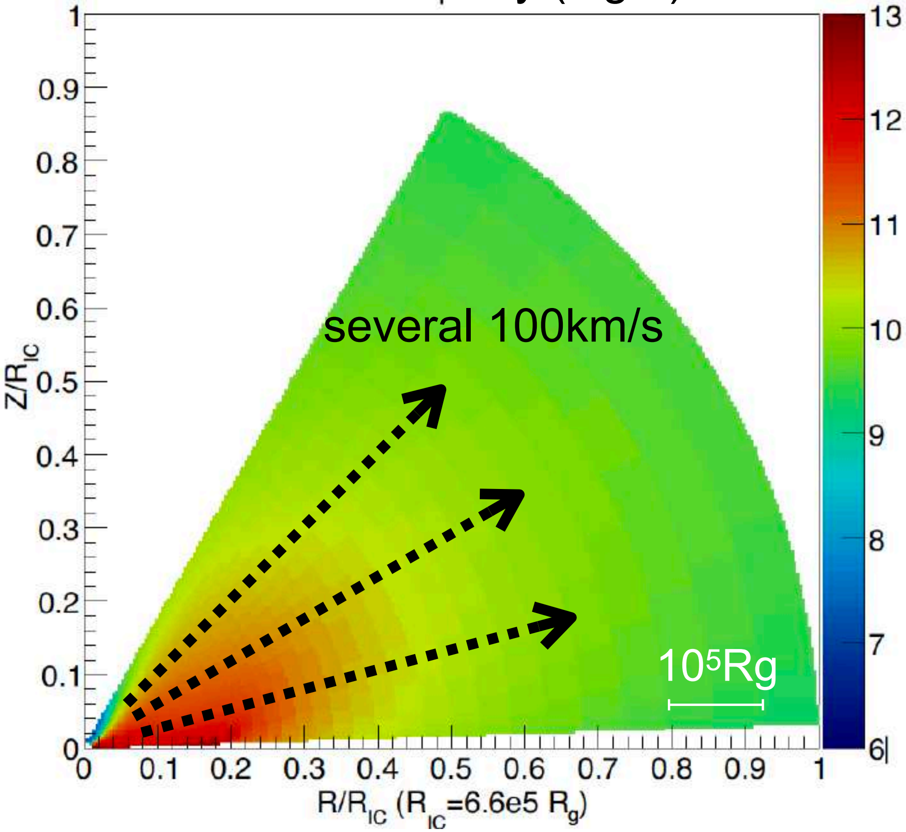

Gas is heated up via the Comptonization and blown away by the gas pressure force and the radiation force.

Monte Carlo Radiation Transfer (MONACO):

viewing angle=45°

60°

75°

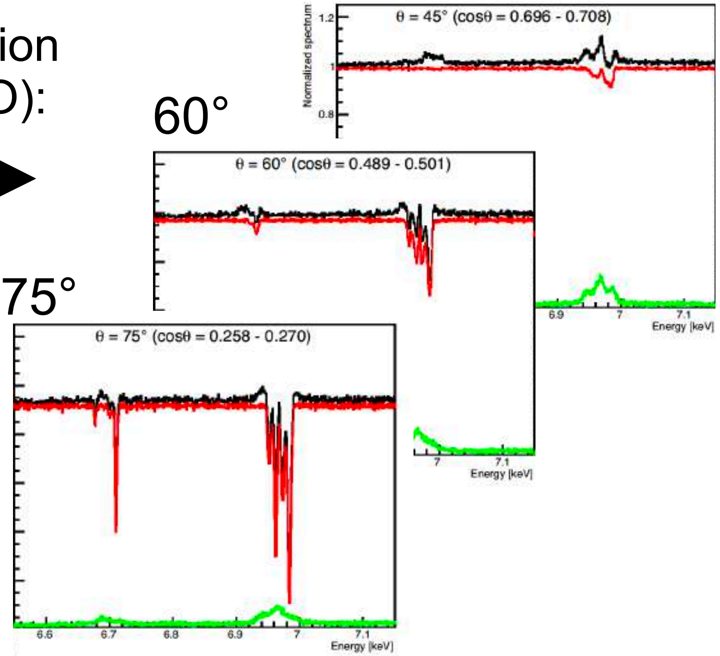

Absorption features (Fe XXVI Ly α_1 & Ly α_2) are obtained

Comparison with observations (H1743-322)

Chandra/HETGS data
with best-fitting model

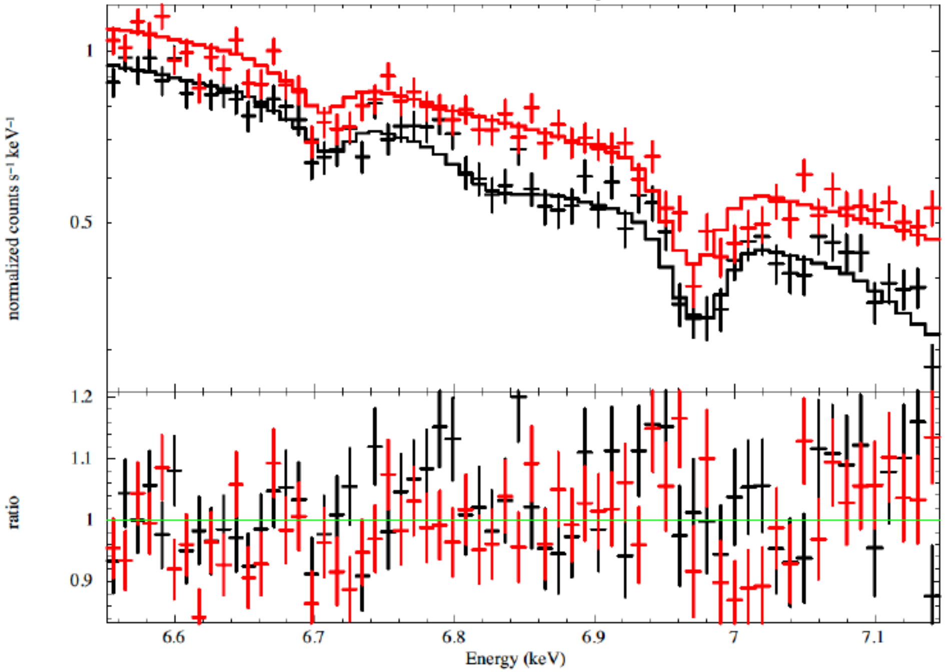

Simulated spectrum of
a 30 ks XRISM observation

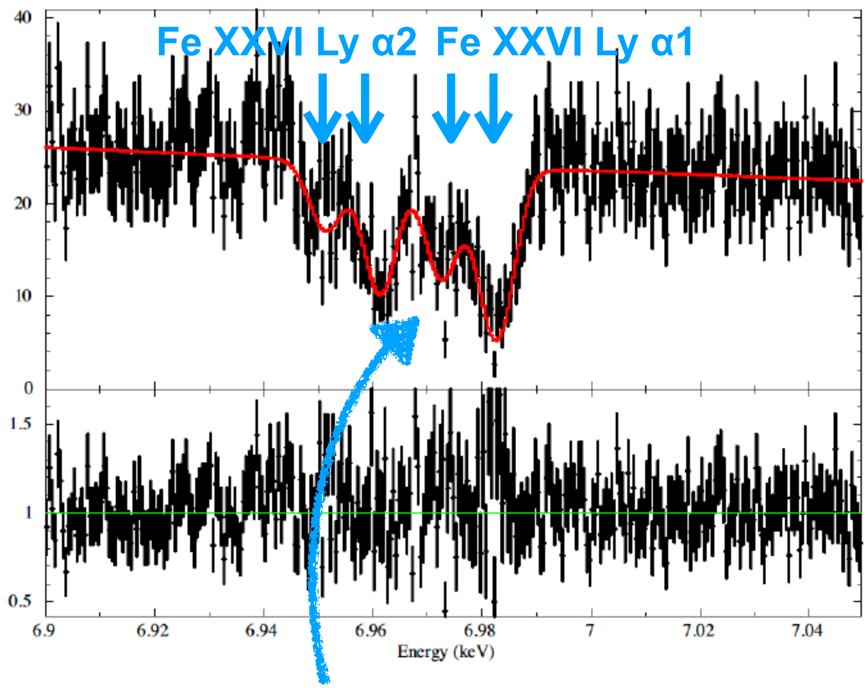

Simulation results are
consistent with observations of
BH binary, H1743−322.

Separation of Fe absorption lines due to velocity difference would be detected by XRISM.

Summary

Super-Eddington case:

Our radiation-MHD simulations reveal that the super-Eddington flows consist of the [1]radiation pressure-supported disk, [2]the radiatively-driven high-velocity outflows around toe rotation axis, and [3]clumpy disk winds with wide opening angle. Basic features of ULXs can be explained by super-Eddington flows.

BH spin enhance the energy-conversion efficiency. This is probably caused by BZ effect. LT precession occurs even in the super-Eddington flows. The precession motion might be origin of QPOs of ULXs.

Near-Eddington case:

Due to the line force, the disk winds are launched from the near-Eddington disks around supermassive BHs. The UFOs observed in AGNs can be explained by line-driving wind. Future X-ray observations are important to reveal the disk wind structure.